An improved solar cell circuit model for organic solar cells

B. Mazhari[*]

*Department of Electrical Engineering and Samtel Center for Display Technology,
Indian Institute of Technology, Kanpur 208016, India*

Abstract

The validity of conventional circuit model for interpreting results obtained using organic solar cells is examined. It is shown that the central assumption in the model that photo-generated current remains constant from short-circuit to open-circuit condition may not hold for organic cells. An improved model based on the photovoltaic response of organic solar cells is proposed and a method of extracting the parameters of the model is presented.
Ⓒ 2005 Elsevier B.V. All rights reserved.

Keywords: Modeling; Organic solar cells; Equivalent circuit; Bilayer

1. Introduction

Organic photovoltaic devices have been actively pursued over the last two decades due to their several potential advantages over traditional silicon-based solar cells including low-cost fabrication using roll-to-roll processing over conformable substrates [1–3]. In order to become a viable alternative, the power conversion efficiency of organic solar cells must approach close to typical efficiencies of 10% reported for thin film amorphous silicon solar cells [4].

---

[*]Tel.: +91 512 2597924; fax: +91 512 2590063.

E-mail address: baquer@iitk.ac.in.

One of the main cause of differences between the structure and operation of organic and inorganic solar cells is that absorption of light creates excitons in most organic semiconductors instead of free electrons and holes. Since the binding energy of excitons is significant, very few of them are able to dissociate at typical values ($\sim 10^6$ V/cm) of built-in electric fields of the cell. As a result, the simplest organic photovoltaic cell consisting of a single layer of organic semiconductor sandwiched between two contacts shows very low efficiency [5,6]. This problem can be overcome through the use of a bilayer device structure consisting of a donor and an acceptor layer. Excitons generated in the donor layer can diffuse to the donor–acceptor (D/A) interface and dissociate to form free electrons and holes. The use of this approach allowed Tang in 1986 to obtain power conversion efficiencies close to $\sim 0.95\%$ [7]. Although, efficiencies as large as $\sim 2.7\%$ have been recently reported in a heterojunction based on Pentacene and C60 [8], a single heterojunction solar cell suffers from a fundamental problem that typical exciton diffusion lengths are considerably smaller than the thickness required for efficient absorption of light. This means that only a fraction of photo-generated excitons can reach the D/A interface to generate free carriers resulting in low quantum efficiency. To overcome this problem, bulk heterojunctions [9–11] consisting of an interpenetrating network of donor and acceptor materials have been used to ensure that all photo-generated excitons find a D/A interface within a diffusion length. Efficiencies as high as 3% have been reported from polymer [12] and $\sim 3.6\%$ from small molecule-based photovoltaic cells [13].

Although significant improvement in power conversion efficiency has been obtained, the efficiencies attained so far are still comparatively low and there is scope for further improvement in all three factors that impact power conversion efficiency namely, short-circuit current, open-circuit voltage and fill factor [1]. An equivalent circuit model is helpful in understanding and optimization of solar cells by providing a quantitative estimate for losses in the device. Although developed in the context of inorganic solar cells [14], the conventional circuit model shown in Fig. 1 has been used to interpret results obtained with organic solar cells as well [2,8,15]. In view of the fact that photovoltaic response in organic solar cells is considerably different from that in inorganic solar cells, the validity of conventional solar cell circuit model is examined in this article. The rest of the paper is organized as follows; in Section 2 the validity of conventional solar cell circuit model is examined. In Section 3, an improved circuit model is proposed and a methodology for parameter extraction is described, which is illustrated using simulation results in Section 4. Finally, the conclusions are summarized in Section 5.

2. Conventional solar cell circuit model

Fig. 1a shows an equivalent circuit model which is commonly used to interpret characteristics of inorganic solar cells. The core of the model consists of photo-generated current I_L connected in parallel with a diode which represents current–voltage characteristics under dark condition. Resistances R_S and R_{SH}
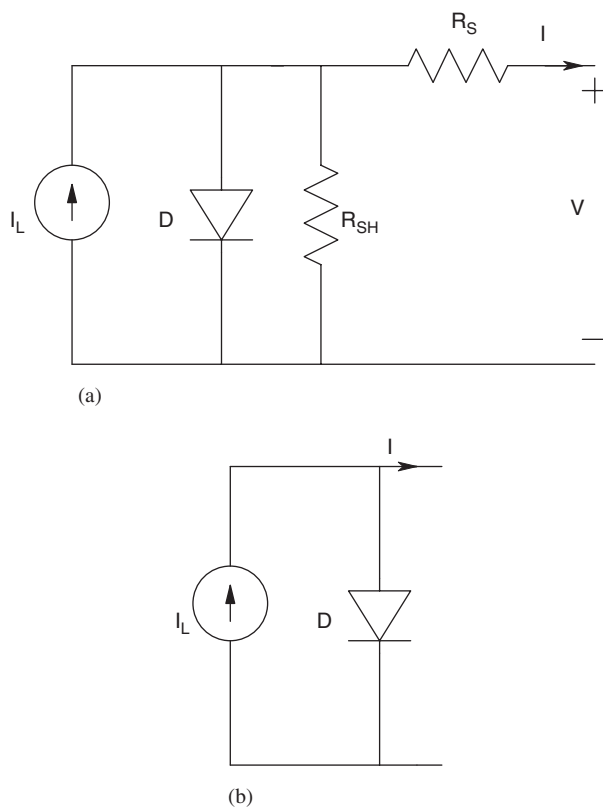
Fig. 1. (a) Conventional equivalent circuit model of solar cell with series resistance R_S and shunt resistance R_{SH}. I_L represents the photo-generated current and diode D represents the characteristics of the device in dark. (b) Ideal model in the absence of parasitic resistances.

represent parasitic series and shunt resistances. The ideal solar cell model in the absence of these resistances is shown in Fig. 1b. For this ideal solar cell, the externally measured current can be related to voltage through the following expression:

$$I = I_L - f(V), \tag{1}$$

where $f(V)$ represents the dark I–V characteristics of the device. Under this model, the short-circuit current (I_{SC}) is simply equal to I_L and open-circuit voltage can be obtained through the expression

$$f(V_{OC}) = I_L. \tag{2}$$

A central assumption in the conventional model is that photo-generated current I_L is constant for given incident light intensity and is independent of voltage. Although this approximation is reasonable for inorganic solar cells, this assumption does not hold for organic solar cells in general. A more general model for organic solar cell is

one where photo-generated current I_L is also a function of voltage. In order to demonstrate the validity of this assertion, let us consider the open-circuit condition described by Eq. (2) which can be written in a more general form as

$$f(V_{OC}) = I_L(V_{OC}). \tag{3}$$

Consider two extreme cases under which the equality described by Eq. (3) can be satisfied;

$$f(V_{OC}) = I_L(V_{OC}) = I_{SC}, \tag{4}$$

$$f(V_{OC}) = I_L(V_{OC}) \ll I_{SC}. \tag{5}$$

The first case described by Eq. (4) corresponds to the traditional case where I_L is a constant. The second extreme case corresponds to the case where photo-generated current varies with voltage and its value at open-circuit condition is negligible compared to short-circuit condition. In this extreme case, the open-circuit condition occurs more due the photo-generated current decreasing to zero by itself. The response of actual organic solar cells is likely to be intermediate between these two extreme states and can be characterized through the parameter ξ

$$\xi = f(V_{OC})/I_{SC}. \tag{6}$$

If $\xi \sim 1$ then the conventional circuit model for organic solar cell can be considered to be valid while if ξ departs significantly from unity then use of such a model is questionable. As an example, consider a polymer solar cell obtained through a blend of MEH-PPV and fullerene derivative PCBM reported by Salima et al. [16]. The solar cell had a power conversion efficiency of 2.9%, short-circuit current density of $8.4\,\text{mA/cm}^2$ and open-circuit voltage of 0.87 V. The dark current at open-circuit voltage ($f(V_{OC})$) was $\sim 1\,\text{mA/cm}^2$ yielding $\xi = 0.119$ which is far less than unity. It is difficult to account for this behavior using series and shunt resistances in the conventional model. As an example, consider the fact that at a voltage of 0.4 V, the current in the external circuit is only $\sim 7\,\text{mA/cm}^2$ [16] as schematically illustrated in Fig. 2. In the conventional model, the photo-generated current remains constant at
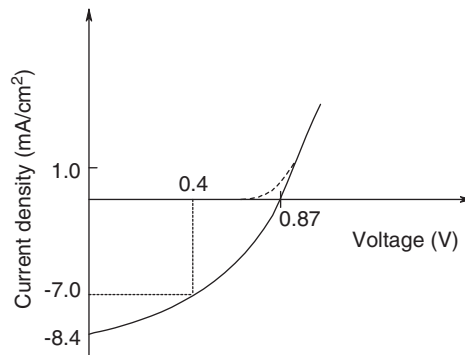

Fig. 2. Schematic diagram showing a typical current–voltage characteristics of an organic solar cell under light (solid line) and under dark (dashed line).

$8.4 \, \text{mA/cm}^2$ which implies that

$$f(0.4 + 7 \times 10^{-3} \times R_S) = 8.4 - 7 = 1.4 \, \text{mA/cm}^2. \tag{7}$$

In writing Eq. (7), we have assumed that shunt resistance is same under light and dark conditions and thus its contribution can be included in the function $f(V)$ without any loss of generality. Noting that the sum $0.4 + 7 \times 10^{-3} \times R_S$ in Eq. (7) cannot exceed the open-circuit voltage and that dark current at open-circuit voltage is only $1 \, \text{mA/cm}^2$, one can see the inadequacy of conventional model in explaining the drop in current with increase in voltage as illustrated in Fig. 2. A different value of parasitic resistances under dark and light conditions may be able to fit the experimental data but in the absence of physical justification, these resistances would just be curve-fitting parameters without any physical significance. In the next section, we show that these results can be readily explained if we allow for the fact that photo-generated current in organic solar cells is not constant but can vary with the external voltage.

3. Proposed organic solar cell circuit model

3.1. General model

The main difference between inorganic and organic solar cells is that following absorption, instead of free carriers, excitons are created [17,18]. These excitons diffuse to the nearest D/A interface and dissociate to form polaron-pairs. The polaron pairs can either recombine or dissociate into free carriers and be subsequently extracted by the electrodes through a drift–diffusion process. In this photovoltaic process, it is more appropriate to consider polaron-pair generation rate as constant for a given light intensity rather than the current. The current depends on competition between polaron recombination and its dissociation and collection by the electrodes. Since the charge collection or extraction efficiency depends on internal electric field, it is expected that current would, in general, depend on voltage across the device. A solar cell circuit model, in the absence of extrinsic series/shunt resistances, that better describes the photovoltaic response of organic solar cells is shown in Fig. 3. I_P describes the net polaron generation rate and is taken as constant for a fixed light intensity. Diode $D_{\text{rec.}}$ models the loss of polarons due to recombination and diode $D_{\text{ext.}}$ models the extraction of free carriers following the dissociation of polarons. Diode D_{dark} models the current–voltage characteristics of the device in the absence of light. There are two reasons for modeling polaron recombination and charge extraction in terms of diodes. Firstly, their use in the manner indicated means that they have an impact only in the presence of light which can forward bias them. Under dark, these diodes would be reverse biased and thus not have any impact on external current–voltage characteristics which would be determined by diode D_{dark} alone. The second reason for use of diodes is that both polaron recombination and charge extraction are likely to have a non-linear characteristics. The proposed model can help explain qualitatively many features
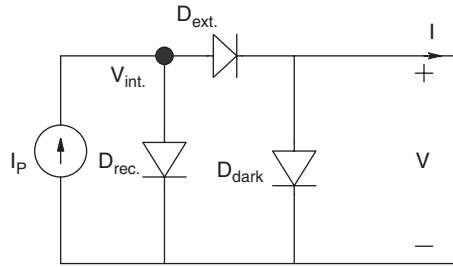
Fig. 3. Proposed equivalent circuit model for organic solar cell in the absence of parasitic series and shunt resistances. I_P represents polaron-pair generation rate and is considered constant for a fixed light intensity. D_{rec} represents loss due polaron-pair recombination and D_{ext} models polaron-pair dissociation and collection of free carriers by electrodes. D_{dark} models the current–voltage characteristics under dark condition.

observed in the characteristics of organic solar cells. Using the model shown in Fig. 3, the current–voltage characteristics under light can be written as

$$I = I_P - I_{rec.} - f(V),\tag{8}$$

$$I_{rec.} = f_{rec.}(V_{int.}),\tag{9}$$

where $f(V)$ represents the dark I–V characteristics and $f_{rec.}$ represents the I–V characteristics for the diode $D_{rec.}$. The short-circuit current can be determined using the following expressions:

$$I_{SC} = I_P - f_{rec.}(V_{int.}),\tag{10}$$

$$I_{SC} = f_{ext.}(V_{int.}),\tag{11}$$

where $f_{ext.}$ represents the I–V characteristics for the charge extraction diode $D_{ext.}$. For small internal electric field or low charge carrier mobilities, there would be significant drop across the diode $D_{ext.}$ which would raise the value of internal voltage $V_{int.}$. This would increase loss due to polaron-pair recombination and reduce short-circuit current according to Eq. (10). Application of reverse bias would reduce $V_{int.}$ and thereby reduce recombination and increase current in the circuit. Eventually, when $V_{int.}$ becomes small enough or negative, the diode $D_{rec.}$ would switch off and current would saturate to its maximum value equal to I_P. Eq. (8) also shows that as the solar cell is forward biased, the current may decrease significantly even if dark current at the applied voltage is negligible. The reason is that an increase in external voltage increases $V_{int.}$ resulting in greater recombination loss through the diode $D_{rec.}$. The open-circuit voltage is determined by the following two equations:

$$I_P = f_{rec.}(V_{int.}) + f(V_{OC}),\tag{12}$$

$$f(V_{OC}) = f_{ext.}(V_{int.} - V_{OC}),\tag{13}$$

Eq. (12) shows that maximum open-circuit voltage would be obtained when internal polaron-recombination is small so that $f_{rec.}(V_{int.}) \ll f(V_{OC})$ and $I_P = f(V_{OC})$. This

corresponds to parameter ξ being close to unity. Besides properties of the D/A interface, polaron recombination would also be lowered by decreasing $V_{\text{int.}}$ through use of materials with higher mobilities.

Although the model shown in Fig. 3 is helpful in providing a qualitative understanding of organic solar cell characteristics, use of diodes as circuit elements complicates a quantitative evaluation of model parameters. In the next section, we describe a simplified model where losses due to polaronic recombination and charge extraction are modeled as resistances so that their values can be extracted relatively easily.

3.2. Simplified model and parameter extraction

Fig. 4 shows the simplified model where loss due to polaron-pair recombination at D/A interface is modeled using shunt resistance $R_{\text{sh}}^{\text{int.}}$ and the difficulty encountered in extracting the charge to the electrodes is modeled by series resistance $R_{\text{S}}^{\text{int.}}$. The superscript 'int.' is used to distinguish these resistances as internal to the device as compared with conventional series resistance which is extrinsic in nature. The diodes D_1 and D_2 are 'ideal' diodes that act like short circuit under forward bias and open circuit under reverse bias. These are included so that the internal series and shunt resistances come into effect only under the presence of light. Although, both internal resistances can, in general, be functions of externally applied voltage and non-linear in nature, we model shunt resistance as constant and series resistance as a variable depending on the magnitude of current across it. As a first order approximation, it is reasonable to assume that polaronic recombination depends more on properties of D/A interface and less on internal electric field as opposed to charge extraction process which would depend strongly on internal electric field and thus the external voltage.

The use of resistances instead of diodes in the model makes extraction of these parameters relatively easier. The current source I_P is simply equal to short-circuit
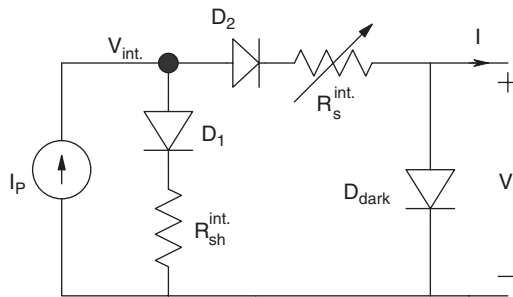

Fig. 4. Simplified equivalent circuit model for organic solar cells in which losses are modeled in terms of resistances. $R_{\text{sh}}^{\text{int.}}$ represents loss due to polaron recombination and $R_{\text{s}}^{\text{int.}}$ models charge extraction to the electrodes. Diodes D_1 and D_2 are ideal diodes that are like short circuit under forward bias and open circuit under reverse bias.
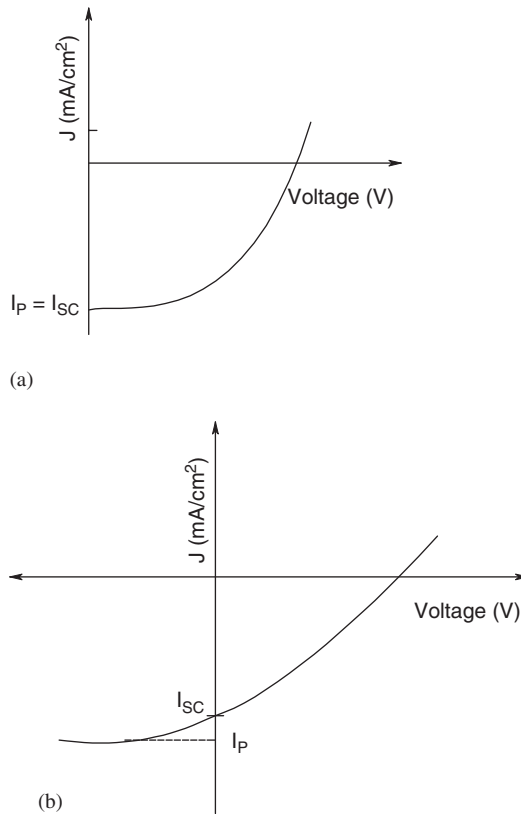
(a)

(b)

Fig. 5. Schematic representation of current–voltage characteristics of solar cell under light showing (a) good saturation and (b) poor saturation at short-circuit condition. I_P represents net polar-pair generation rate and I_{SC} represents short-circuit current.

current I_{SC} if the current shows good saturation near the short-circuit condition as illustrated in Fig. 5a. On the other hand if current does not show saturation as illustrated in Fig. 5b, then a negative voltage can be applied till the current saturates to a constant value. As discussed earlier, application of negative voltage reduces $V_{int.}$ and polaronic losses eventually making it negligible. The shunt resistance $R_{sh}^{int.}$ can be determined if a voltage V_X could be found where current under dark and light are almost equal to each other as illustrated in Fig. 6. Under this condition, current through the series resistance $R_S^{int.}$ is negligible so that $V_X \cong V_{int.}$ and current through $R_{sh}^{int.}$ is simply I_P so that

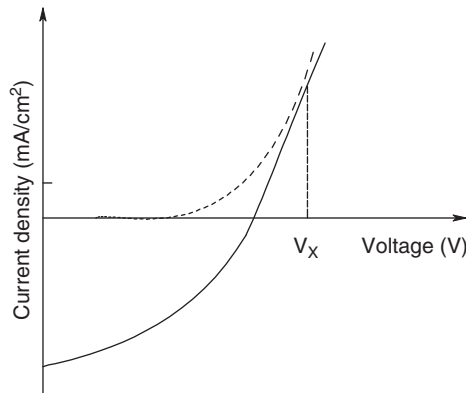$$R_{sh}^{int.} \cong \frac{V_X}{I_P}. \tag{14}$$

Fig. 6. Schematic diagram illustrating voltage V_X at which current under dark and light conditions is approximately equal.

Having extracted values of I_P and $R_{sh}^{int.}$, the series resistance $R_S^{int.}$ as a function of current can be determined using the following expression:

$$R_s^{int.} = \frac{(I_P - I - f(V))R_{sh}^{int.} - V}{I_P - I - f(V)}. \tag{15}$$

The first term in the numerator represents the magnitude of internal voltage $V_{int.}$ and the denominator represents the net current flowing through the series resistance. In the next section, we illustrate extraction of these parameters using simulation results.

4. Simulation results and discussion

For illustration of the parameter extraction process, a single heterojunction solar cell shown in Fig. 7a was considered. The current–voltage characteristics under dark and light were obtained through numerical simulations carried out using SimWindows [19], a light-emitting diode and solar cell simulator based on standard drift–diffusion formalism in the bulk and thermionic emission at the contacts and heterojunctions. To model polaron-pair generation/recombination, a thin interfacial layer (thickness $\sim$20 Å) is introduced between donor and acceptor layers with energy level alignment as illustrated in Fig. 7b. Optical generation is confined only to this thin interfacial layer. Once electron–hole pairs are generated in this layer, the electrons find it energetically favorable to go to EAL and holes to EDL. As a result, only electrons are created in EAL and holes in EDL and currents are monopolar in these regions like in a real device. Polaron recombination is modeled through bimolecular and Shockley-Hall-read recombination lifetimes. Although the thermionic emission model used for describing injection into organic semiconductor and polaron-pair generation/recombination modeled in the simulation are simplistic, the
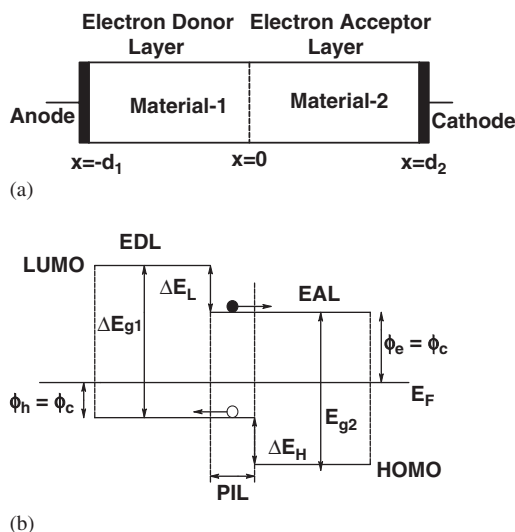
Fig. 7. (a) Schematic diagram of a single heterojunction solar cell. (b) Energy level diagram at equilibrium showing the relevant energy levels. ϕ_c represents electron and hole injection barrier heights taken to be equal. E_{g1} and E_{g2} represent energy gaps of donor and acceptor layers, respectively. ΔE_L and ΔE_H represent discontinuity in LUMO and HOMO levels, respectively, at the heterojunction. PIL is the interfacial 'polaronic' layer which is introduced between EDL and EAL layers to model polaron-pair generation and recombination.

simulation results are only used as illustrations and conclusions derived from them are not dependent on the details of the simulation and are valid in general.

Fig. 8 shows an example of current–voltage characteristics obtained through numerical simulations. One can notice that the current under illumination shows poor saturation near short-circuit condition due to low carrier mobilities (10^{-5} cm^2/Vs) assumed in simulations. However, on application of reverse bias the current saturates to a constant value as illustrated in the inset of Fig. 8. This also yields an estimate for the value of $I_P = 14.6$ mA/cm^2 as discussed earlier. A shunt resistance of $R_{sh}^{int.} = 83.6\,\Omega\,\text{cm}^2$ was extracted using Eq. (14) with a value of $V_X = 1.22$ V. The series resistance was next extracted using Eq. (15) and is shown as a function of voltage in Fig. 9. The series resistance increases from a value of $\sim 22\,\Omega\,\text{cm}^2$ at short-circuit condition to as large as $\sim 900\,\Omega\,\text{cm}^2$ near open-circuit voltage of 0.92 V. As explained earlier, this increase in series resistance represents reduction in internal electric field causing charge extraction to the electrodes increasingly difficult. Fig. 10 shows a comparison of current–voltage characteristics under light obtained from simulations with that obtained using the equivalent circuit model with extracted values of resistances. The excellent match between the two characteristics indicates the validity of the parameter extraction process. Fig. 11a shows another current–voltage characteristics that was obtained under identical simulation conditions as results shown in Fig. 8 except that carrier mobilities were two orders
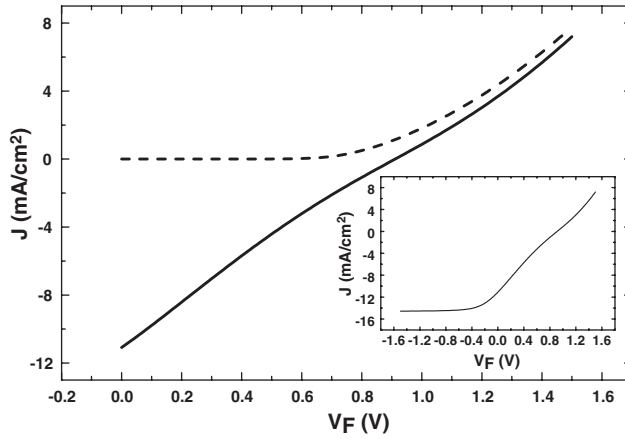
Fig. 8. Current–voltage characteristics under dark (dashed line) and under illumination (solid line) for a bilayer organic solar cell obtained through numerical simulations. Results shown are for $E_{g1} = E_{g2} = 2\,\text{eV}$; $\Delta E_H = \Delta E_L = 0.5\,\text{eV}$. The electron and hole mobilities in both layers were equal to $10^{-5}\,\text{cm}^2/\text{Vs}$. The thickness of polaronic layer was $20\,\text{Å}$ and polaron-pair generation rate of $9 \times 10^{16}\,\text{cm}^{-2}\,\text{s}^{-1}$ and polaron recombination lifetime of $10\,\mu\text{s}$ was assumed. The electron and hole injection barrier heights (ϕ_C) were taken as $0.3\,\text{eV}$. The inset shows the current–voltage characteristics under illumination when the solar cell is reverse biased.
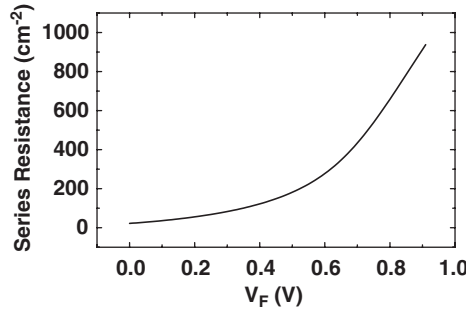

Fig. 9. Internal series resistance ($R_S^{\text{int.}}$) extracted from the results shown in Fig. 8 as a function of external voltage.

of magnitude higher at $10^{-3}\,\text{cm}^2/\text{Vs}$. The current now shows excellent saturation and a high fill factor. $I_P = 14.6\,\text{mA/cm}^2$ and a shunt resistance of $R_{sh}^{\text{int.}} = 83.6\,\Omega\,\text{cm}^2$ was extracted from the characteristics. The extracted series resistance is shown in Fig. 11b. As expected, the series resistance now is very low increasing only to a value of $\sim 10\,\Omega\,\text{cm}^2$ near open-circuit condition.

We have so far discussed extraction of internal series and shunt resistances. Depending on the nature of device, the extrinsic series and shunt resistances may also have a significant impact on solar cell characteristics, especially in well optimized devices where internal resistances are small. A better parameter extraction
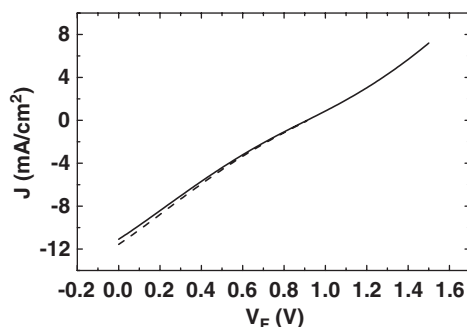
Fig. 10. Comparison of current–voltage characteristics under illumination obtained using numerical simulations (solid line) with that obtained through use of equivalent circuit model (dashed line) with parameters extracted from characteristics shown in Fig. 8.
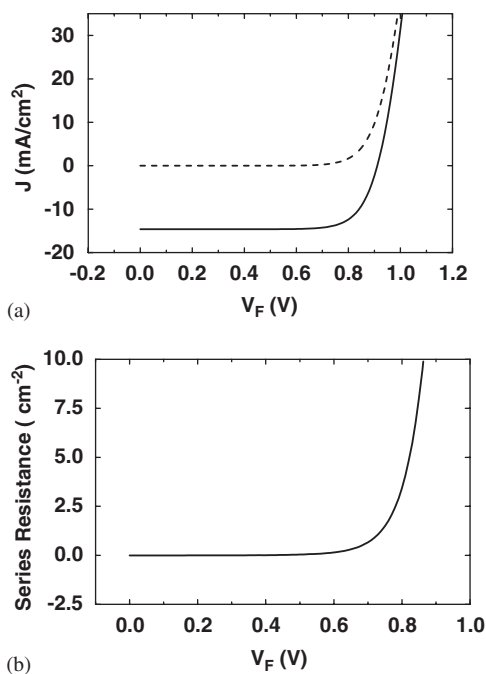

(a)

(b)

Fig. 11. (a) Current–voltage characteristics under dark (dashed line) and under illumination (solid line) for a bilayer organic solar cell obtained through numerical simulations. Simulation conditions were same as that for Fig. 8 except that the electron and hole mobilities in both layers are equal to 10^{-3} cm^2/Vs; (b) internal series resistance ($R_S^{int.}$) extracted from the results shown in Fig. 11a as a function of external voltage.

methodology is needed which can decouple not only the effects of internal and external resistances but also consider them as functions of voltage and incident light intensity.

5. Conclusions

In summary, we have shown that conventional solar cell circuit models are inadequate for describing behavior of organic solar cells because the assumption that photo-generated current is constant from short-circuit to open-circuit condition is not valid in general. An improved circuit model based on the photovoltaic response of organic solar cells has been proposed which can better explain the characteristics of these devices. A methodology for extracting parameters for a simplified model has been outlined and illustrated through simulation results.

References

[1] P. Peumans, A. Yakimov, S.R. Forrest, J. Appl. Phys. 93 (2003) 3693.
[2] H. Hoppe, N.S. Sariciftci, J. Mater. Res. 19 (2004) 1924.
[3] K. Yoshino, K. Tada, A. Fujii, E.M. Conwell, A. Zakhidov, IEEE Trans. ED 44 (1997) 1315.
[4] R.E.I. Schropp, M. Zeman, IEEE Trans. ED 46 (1999) 2086.
[5] G.A. Chamberlain, Sol. Cells 8 (1983) 47.
[6] D. Wohrle, D. Meissner, Adv. Funct. Mater. 3 (2001) 129.
[7] C.W. Tang, Appl. Phys. Lett. 48 (1986) 183.
[8] S. Yoo, B. Domercq, B. Kippelen, Appl. Phys. Lett. 85 (2004) 5427.
[9] G. Yu, J. Gao, J. Hummelen, F. Wudl, A.J. Heeger, Science 270 (1995) 1789.
[10] F. Padinger, R.S. Rittberger, N.S. Sariciftci, Adv. Funct. Mater. 13 (2003) 85.
[11] P. Peumans, S. Uchida, S.R. Forrest, Nature (London) 425 (2003) 158.
[12] Y. Kim, S.A. Choulis, J. Nelson, D.D.C. Bradley, S. Cook, J.R. Durrant, Appl. Phys. Lett. 86 (2005) 63502.
[13] S. Uchida, J. Xue, B.P. Rand, S.R. Forrest, Appl. Phys. Lett. 84 (2004) 4218.
[14] S.M. Sze, Physics of Semiconductor Devices, second ed., Wiley, New York.
[15] J.M. Nunzi, C. R. Physique 3 (2002) 523.
[16] A. Salima, R.D. Bettignies, J.M. Nunzi, Appl. Phys. Lett. 84 (2004) 2178.
[17] J.A. Barker, C.M. Ramsdale, N.C. Greenham, Phys. Rev. B 67 (2003) 75205.
[18] B.A. Gregg, J. Phys. Chem. B 107 (2003) 4688.
[19] D.W. Winston, R.E. Hayes, IEEE J. Quantum Electron. 34 (1998) 707.